NASA Technical Memorandum 4784

An Experimental Study of Fatigue Crack Growth in Aluminum Sheet Subjected to Combined Bending and Membrane Stresses

Edward P. Phillips
Langley Research Center • Hampton, Virginia

National Aeronautics and Space Administration
Langley Research Center • Hampton, Virginia 23681-2199

October 1997

Available electronically at the following URL address: http://techreports.larc.nasa.gov/ltrs/ltrs.html

Printed copies available from the following:

NASA Center for AeroSpace Information
800 Elkridge Landing Road
Linthicum Heights, MD 21090-2934
(301) 621-0390

National Technical Information Service (NTIS)
5285 Port Royal Road
Springfield, VA 22161-2171
(703) 487-4650

Abstract

An experimental study was conducted to determine the effects of combined bending and membrane cyclic stresses on the fatigue crack growth behavior of aluminum sheet material. The materials used in the tests were 0.040-in.-thick 2024-T3 alclad and 0.090-in.-thick 2024-T3 bare sheet. In the tests, the membrane stresses were applied as a constant amplitude loading at a stress ratio (minimum to maximum stress) of 0.02, and the bending stresses were applied as a constant amplitude deflection in phase with the membrane stresses. Tests were conducted at ratios of bending to membrane stresses (B/M) of 0, 0.75, and 1.50. The general trends of the results were for larger effects of bending for the higher B/M ratios, the lower membrane stresses, and the thicker material. The addition of cyclic bending stresses to a test with cyclic membrane stresses had only a small effect on the growth rates of through-thickness cracks in the thin material, but had a significant effect on the crack growth rates of through-thickness cracks in the thick material. Adding bending stresses to a test had the most effect on the initiation and early growth of cracks and had less effect on the growth of long through-thickness cracks.

Introduction

Fatigue cracking in aircraft fuselage skin joints has been a topic of considerable interest to airframe manufacturers, aircraft operators, and regulatory agencies in recent years. The subject is of particular interest to those responsible for assessing and ensuring the continued airworthiness of aircraft fleets that have been in service for a long time. The research community has been challenged to provide the methodology necessary to predict the fatigue crack growth behavior of the joints. To develop the required methodology, potential shortcomings of current methodology must be explored to aid in the development of improvements. One area requiring investigation concerns the effect of local bending in the joints on the crack growth behavior. Strain measurements made at a fuselage longitudinal skin joint during fuselage pressurization have shown that significant bending occurs in the skin (refs. 1 and 2), but current crack growth prediction models do not account for the bending stresses. A survey of the literature did not reveal any pertinent experimental studies of the effect of combined bending and membrane stresses on the crack growth behavior of sheet material.

The objectives of the current study were (1) to determine the magnitude of the effect of bending stresses on the crack growth behavior and (2) to provide data that could be used to evaluate the capability of crack growth models to account for the effects of bending stresses. Because of the experimental difficulties involved in running tests in which both the membrane and bending stresses are actively controlled, the tests were conducted with constant-amplitude membrane loading and constant-amplitude bending displacements. Tests were conducted on two sheet thicknesses (0.040 and 0.090 in.) and with ratios of bending to membrane stresses of 0, 0.75, and 1.50. The range of test conditions was selected to span expected conditions in current fuselage structures.

Tests

Materials and Specimens

Tests were conducted on center-cracked specimens made of 0.040-in.-thick 2024-T3 alclad and 0.090-in.-thick 2024-T3 bare aluminum alloy sheet. The long axis of the specimen was perpendicular to the sheet rolling direction. That is, crack growth was determined for the T-L orientation. The specimen configuration is shown in figure 1.

Test Apparatus

Tests were conducted in a conventional, single-actuator servohydraulic testing machine. The testing fixture is shown schematically in figure 2. The figure shows an edge view of the specimen mounted in the fixture. Loads were transmitted into the fixture through pin-clevis connections at the top and bottom grips. The membrane stresses in the specimen were set by controlling the axial load through the pins, and the bending stresses in the specimen were set by varying the eccentricity between the plane of the specimen and the loading line through the pin. A plate (forcing plate) that connected to the grip and extended almost to the test section was used to force the highest bending stresses to occur in the sheet at the test section. The surface of the forcing plate that touched the specimen was coated with Teflon[1] and lubricated with a light grease except in the gripping area. The spring-loaded roller clamp shown near the test

[1] Trademark of E. I. duPont deNemours Company.

section also served to localize the bending at the test section. The springs (restraining springs) shown attached to the forcing plate and an external support were used to ensure that the outer fiber strains in the specimen would vary monotonically with load (discussed further in the following section). Sliding supports at the top and bottom grips prevented side loads from being applied to the load cell or testing machine actuator.

Test Procedures

All fatigue crack growth tests were constant-load amplitude tests that had an applied load ratio (minimum/maximum) of 0.02. Therefore, the membrane stress ratio was also controlled to remain at 0.02 throughout the test. Because the bending was induced by the applied load, the bending and membrane stresses were always in phase (minima and maxima occurring at the same time), but the bending stresses could not be actively controlled during the test. Instead, the test was set up so that the bending displacements remained constant during the test. Measurements confirmed that the bending displacement was not a function of the specimen bending stiffness and that the bending displacement remained constant as the crack grew during the tests.

Before any crack growth tests were run, an unnotched specimen with five pairs (gages on front and back surfaces at same width location) of strain gages spaced across the width at the test section was mounted and loaded to typical test levels. Measured strains confirmed that the strain distribution across the width was uniform and that the membrane strains were consistent with the material modulus and loading level. Checks also were made to confirm that there were no significant dynamic effects on the strains at the test cycling frequency of 2 Hz.

Each test was set up with a pair of front and back strain gages located at each edge of the specimen at the test section. The gages were used to confirm proper alignment and to determine the ratio of bending to membrane strains. The procedure for each test was as follows:

1. The specimen assembly (specimen and grips) was installed in the machine, and the specimen was held in an unstressed, vertical position by an additional fixture until the restraining springs were attached to the forcing plates. The restraining springs resisted any movement of the forcing plates.

2. With the springs in place, the additional fixture was removed and the test minimum load was applied to keep the loading pins in contact with the clevises. The strain gages were zeroed at this condition.

3. Load was applied in increments, and the strains were measured at each step to determine whether the desired alignment and ratio of bending to membrane strains were being attained. Initial setup to achieve a particular strain ratio was based on a calibration curve made with the unnotched specimen. Even so, some adjustments to the test fixture spacers were required in some cases to achieve desired results. Care was taken to ensure that maximum outer fiber strains experienced in test setup did not exceed the test strains.

The variation of strain with load at the outer fibers was not linear, but it was monotonic. A typical example is shown in figure 3 for a test with a ratio of bending to membrane strain of 1.50. Because the bending strain did not vary linearly with load, the ratio of bending to membrane strains also varied during the loading cycle. The tests were set up so that the desired ratio was achieved at the maximum load in the cycle, and because the strain gages were zeroed at the minimum load in the cycle, the ratio of the range in bending strain to the range in membrane strain was the same as the instantaneous value at maximum load.

During the crack growth tests, crack length measurements were made optically with micrometer slides and 60X microscopes. Crack lengths (four locations) and cycles were recorded at approximately every 0.020 in. of growth at each crack tip.

Tests were conducted at several maximum load levels in order to cover a reasonably large range in crack growth rates for each strain ratio and material thickness. Test parameters for each test are listed in table 1.

Results and Discussion

Results for 0.040-In.-Thick 2024-T3 Alclad Sheet

Tests were conducted with B/M of 0, 0.75, and 1.50. The tests without bending (B/M = 0) showed symmetrical crack growth about the specimen longitudinal centerline and the specimen midthickness. In tests with bending, the cracks were symmetrical about the specimen longitudinal centerline, but the cracks did not grow symmetrically about the specimen midthickness. The differences in crack half-length at the two surfaces (normalized by the specimen thickness) are shown in figure 4 plotted against the crack half-length on the high-strain surface. The results for B/M = 0.75 and for B/M = 1.50 are shown in figures 4(a) and 4(b), respectively. The plotted crack half-lengths are the averages of the two lengths measured from the specimen longitudinal centerline on each surface. The cracks started growing on the high-strain surface first and grew for a time as part-through cracks, such that the largest differences in length

Table 1. Fatigue Crack Growth Tests and Test Parameters

[Membrane stress ratio = 0.02; cyclic frequency = 2 Hz; and air at room temperature]

Bending to membrane strain ratio	Test maximum load, lb	Test maximum membrane stress, ksi	Number of tests
0.040-in.-thick 2024-T3 alclad sheet			
0	700	5.8	1
0	800	6.7	1
0	1000	8.3	2
0	1200	10.0	1
0	1600	13.3	1
0.75	800	6.7	1
0.75	1200	10.0	1
1.50	800	6.7	1
1.50	1200	10.0	2
0.090-in.-thick 2024-T3 bare sheet			
0	1800	6.7	1
0	2400	8.9	1
0	3100	11.5	1
0.75	1800	6.7	2
0.75	2400	8.9	1
0.75	3100	11.5	1
1.50	1450	5.4	1
1.50	1800	6.7	2
1.50	2400	8.9	1
1.50	3100	11.5	1

occurred at the start of the tests. After the cracks started growing at the low-strain surface, the cracks at that surface tended to grow faster than those at the high-strain surface, and the length difference between the surfaces gradually decreased (but not to zero) as the cracks grew longer. The tests at B/M = 1.50 always showed greater length differences at a given crack length and test membrane stress than did the tests at B/M = 0.75.

The crack growth rate results for B/M = 0.75 and B/M = 1.50 are shown in figures 5 and 6, respectively. The results for B/M = 0 are also plotted in each figure for comparison. The results are shown as plots of crack growth rate against stress intensity factor range (ΔK), where (1) results are shown only for through cracks, (2) the crack half-length used in computing rates and stress intensity factors was the average of crack lengths measured on both surfaces at both crack fronts (four half-length measurements), (3) rates were calculated with the secant method of ASTM Standard E647 (ref. 3), (4) only the membrane stresses were used to calculate ΔK, and (5) ΔK was calculated with the following expression given in ASTM E647:

$$\Delta K = \Delta P / B \sqrt{(\pi\alpha/2W)\sec(\pi\alpha/2)} \qquad (1)$$

where $\alpha = 2a/W$, a is the crack half-length, W is the specimen width, ΔP is the cyclic load range, and B is the specimen thickness.

The intent of plotting the results in this manner was to illustrate the increase in average crack growth rates that could be caused by the addition of cyclic bending stresses to a cyclic membrane stress test.

The results for B/M = 0.75 in figure 5 show that the addition of bending stresses caused some increase in rate at the lower ΔK levels, but not at higher ΔK values. There was very little effect at values of ΔK greater than 10 ksi-in$^{1/2}$. The results for B/M = 1.5 in figure 6 show the same trends as results for B/M = 0.75, but the increase in rate caused by bending was somewhat larger at the low ΔK values and persisted to a higher ΔK value (about 13 ksi-in$^{1/2}$).

Although the addition of bending did not cause large differences in crack growth rate, the bending did cause shorter overall test lives. This result is shown in figure 7, where the life ratios (life with bending/life without bending) are plotted. Two life ratios are plotted for each test based on (1) cycles to start and grow a crack from the notch to a half-length of 0.7 in. and (2) cycles to grow a through crack from 0.5 to 0.7 in. in half-length. All of the ratios are less than one, indicating an effect of the bending, but only the test at B/M = 1.50 at the low membrane stress showed a substantial reduction in life. In that test, life (initiation and growth to half-length of 0.7 in.) with bending was about one-half that for the test without bending. Comparison of the two life ratios plotted for that test indicates that the bending had the most effect on initiation and early growth of the cracks and had less effect on the growth of the long through-thickness cracks.

Results for 0.090-In.-Thick 2024-T3 Bare Sheet

Tests were conducted with B/M ratios of 0, 0.75, and 1.50. For tests with bending, the differences in crack length on the two surfaces were recorded and analyzed in the same manner as was done for the 0.040-in.-thick material. The results for B/M = 0.75 and for B/M = 1.50 are shown in figures 8(a) and 8(b), respectively. The trends in the results for the 0.090-in.-thick material were similar to those observed for the 0.040-in.-thick material, but the normalized length differences observed for the thicker material were always greater at a given crack length and membrane stress than was observed in the thinner material. For example, tests with B/M = 1.50 on the thin material showed a maximum length difference of about 1.5 sheet thicknesses early in the test, whereas the thicker material showed a difference of about 3.0 thicknesses. Also, in the thicker material, there was a more distinct trend for the length differences during early growth to be a function of test maximum membrane stress. Tests with a lower membrane stress sustained longer part-through cracks before crack growth started on the low-strain surface. The dependence of the crack length differences on membrane stress and the magnitude of the crack length differences decreased as the cracks grew longer. The difference in crack length at the end of a B/M = 1.50 test was typically about 1.0 thickness.

The crack growth rate results for B/M = 0.75 and B/M = 1.5 are shown in figures 9 and 10, respectively. The procedures for analyzing and plotting the data are the same as those described above for the 0.040-in.-thick material. The results for B/M = 0.75 in figure 9 show the same trends that were observed for the thinner material for both B/M ratios. That is, the addition of the bending stresses caused somewhat higher rates at the lower ΔK values, but at higher ΔK values, the rates became the same as for the no-bending case. For the thicker material, the increase in rates was greater and the difference between the bending and no-bending cases persisted to a higher ΔK than was observed for the thinner material.

The results for B/M = 1.50 in figure 10 show a different behavior than that observed in the other tests. Early in the tests, when there was a large difference in crack length at the two surfaces, the tests with bending showed a much larger growth rate than did the tests without bending. This difference was largely caused by the very rapid growth on the low-strain surface just after the crack had started growing on that surface. However, even at long crack lengths after the length difference between the surfaces had stopped changing rapidly, the growth rates of the tests with bending were about twice the rates of the no-bending tests. The difference in growth rates persisted over the entire ΔK range of the data.

As would be expected from the crack growth rate data, the reduction in test lives that resulted from the addition of bending was greater in the 0.090-in. material than in the 0.040-in. material. The life ratios for the tests on the 0.090-in. material are shown in figure 11 in the same way they were shown for the 0.040-in. material in figure 7. As for the thin material, the greatest reduction in life occurred in the test with B/M = 1.5 and the lowest membrane stress level. For this test, the life (initiation and growth to half-length of 0.7 in.) with bending was only about one-third that of the test without bending. The results in figure 11 also show that the bending had more effect on the initiation and initial growth than it did on the growth of long cracks. For the B/M = 1.5 tests, even the growth lives of long through-cracks were reduced significantly by the bending. The other trend evident in figure 11 is that the bending effects were more pronounced in the tests with lower membrane stresses.

Conclusions

An experimental study was conducted to determine the effects of combined bending and membrane cyclic stresses on the fatigue crack growth behavior of aluminum sheet material. The materials used in the tests were 0.040-in.-thick 2024-T3 alclad and 0.090-in.-thick 2024-T3 bare sheet. In the tests, the membrane stresses were applied as a constant amplitude loading at a stress ratio of 0.02, and the bending stresses were applied as a constant amplitude deflection in phase with the membrane stresses. Tests were conducted at ratios of bending to membrane stresses (B/M) of 0, 0.75, and 1.50. The following conclusions were drawn from the results of the tests:

1. The general trends of the results were for larger effects of bending for the higher B/M, the lower membrane stresses, and the thicker material.

2. The effect of adding cyclic bending stresses to a test with cyclic membrane stresses was always to reduce test lives. For the most extreme case, the life of the test with bending was only one-third that of the test without bending. The bending had the most effect on the initiation and early growth of cracks and had less effect on the growth of long through-thickness cracks.

3. The addition of cyclic bending had very little effect on the growth rates of through-thickness cracks in the thin material over most of the growth rate range investigated. Some increase in rates was evident at the lower end of the growth rate range.

4. The bending significantly increased the growth rates of through-thickness cracks in tests of the thick

material at B/M = 1.5. The growth rates were increased by about a factor of two at long crack lengths.

5. The thick material sustained long part-through cracks early in the tests. For the most extreme case, the crack was about 0.3 in. long on one surface before growth started on the other surface.

NASA Langley Research Center
Hampton, VA 23681-2199
June 12, 1997

References

1. Phillips, Edward P.; and Britt, Vicki O.: *Measurements of Fuselage Skin Strains and Displacements Near a Longitudinal Lap Joint in a Pressurized Aircraft.* NASA TM-104163, 1991.

2. Jeong, David Y.; Roach, Dennis P.; Canha, Joseph V.; Brewer, John C.; and Flournoy, Thomas H.: *Strain Fields in Boeing 737 Fuselage Lap Splices—Field and Laboratory Measurements With Analytical Correlations.* DOT-VNTSC-FAA-95-10, U. S. Dept. Transp., June 1995.

3. *Metals Test Methods and Analytical Standards.* Volume 03.01 of the 1995 Annual Book of ASTM Standards, ASTM, 1995, pp. 578–614.

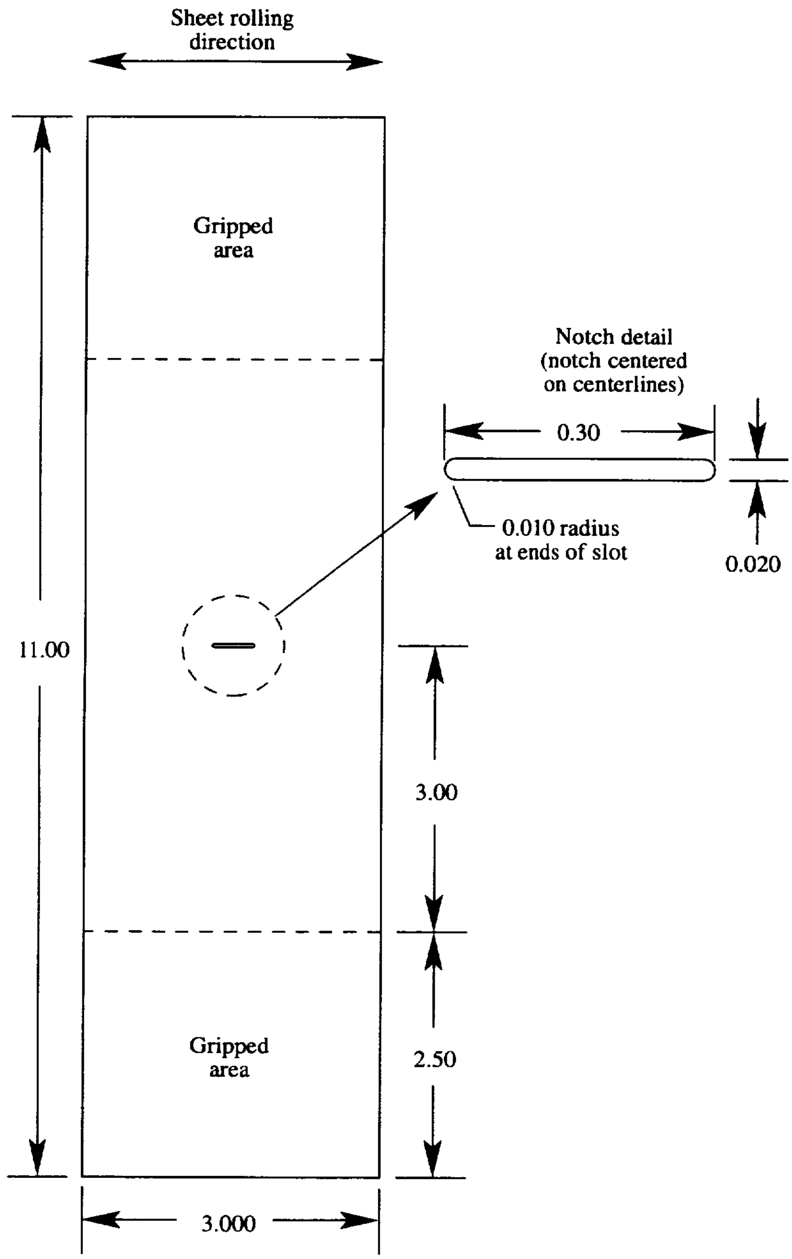

Figure 1. Specimen configuration; dimensions are in inches.

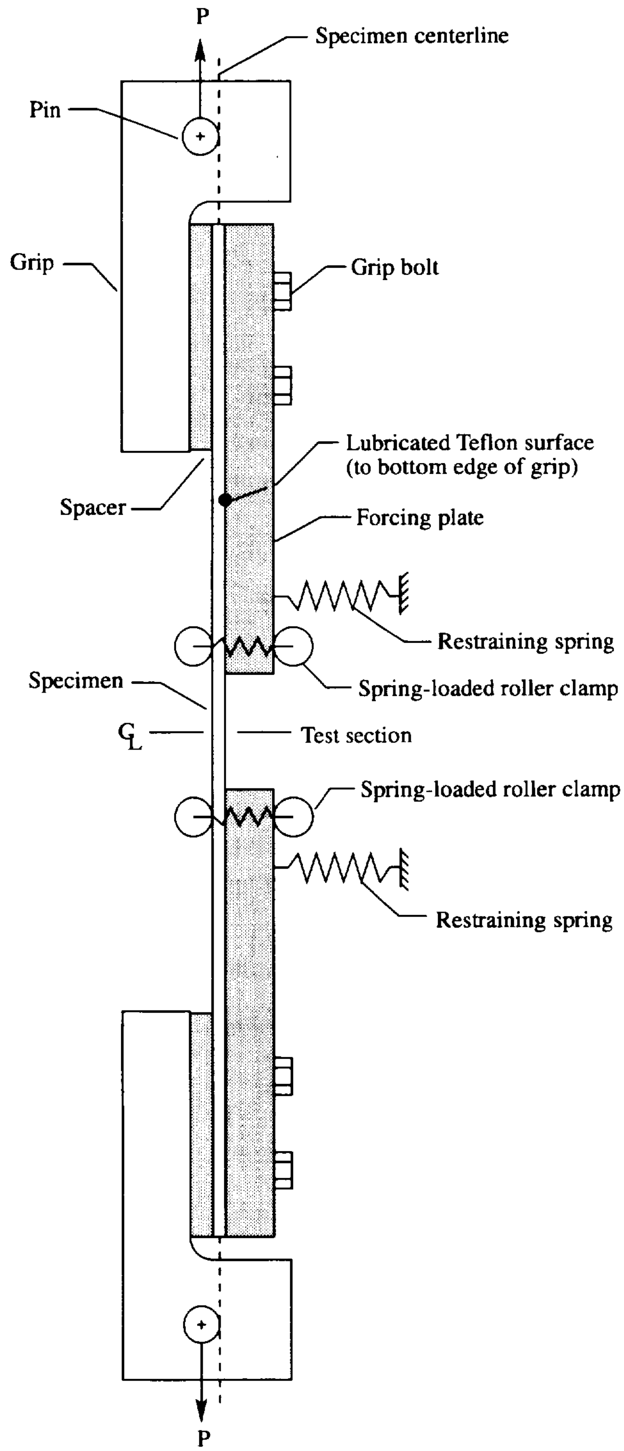

Figure 2. Schematic of testing fixture used to apply combined bending and membrane stresses (edge view).

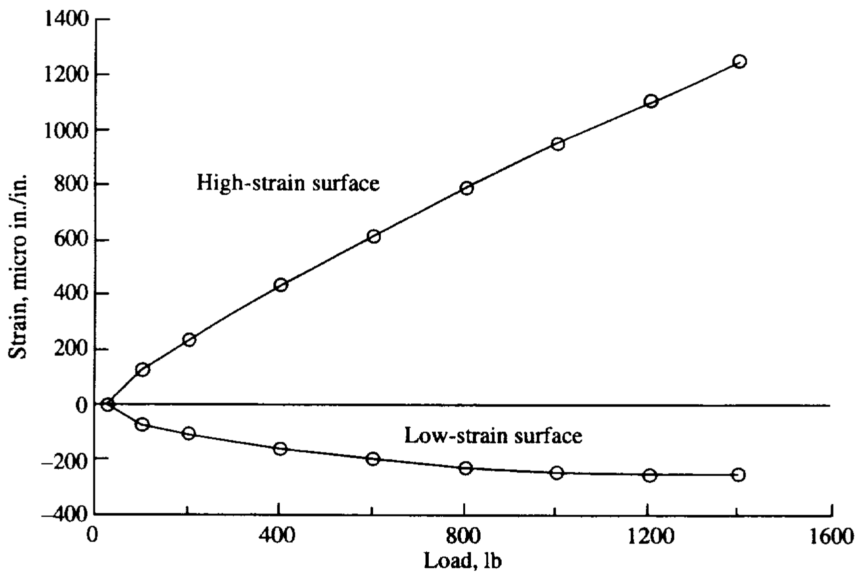

Figure 3. Variation of strain with load in a test with a ratio of bending to membrane strain of 1.50.

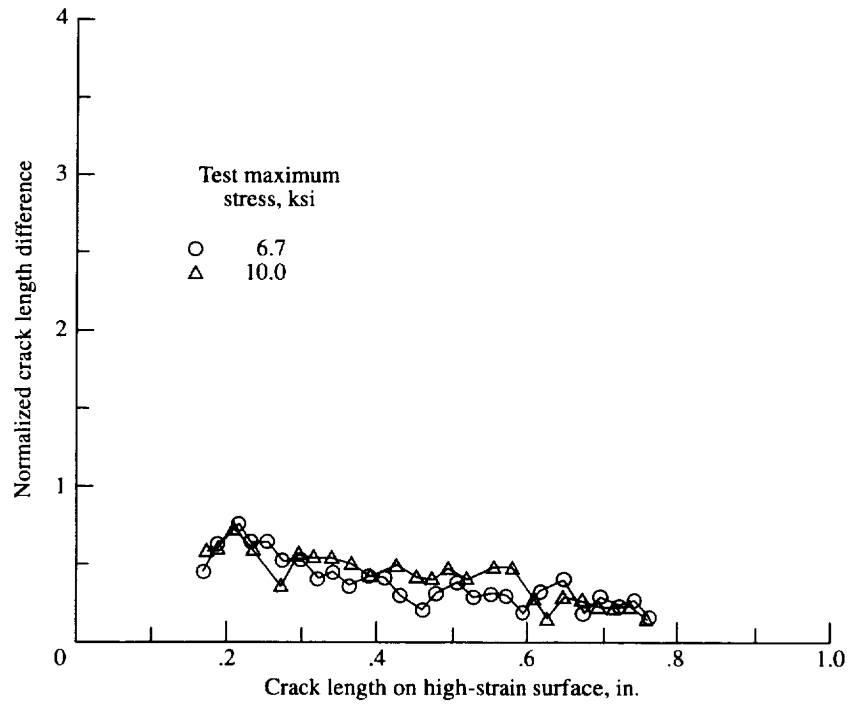

(a) B/M = 0.75.

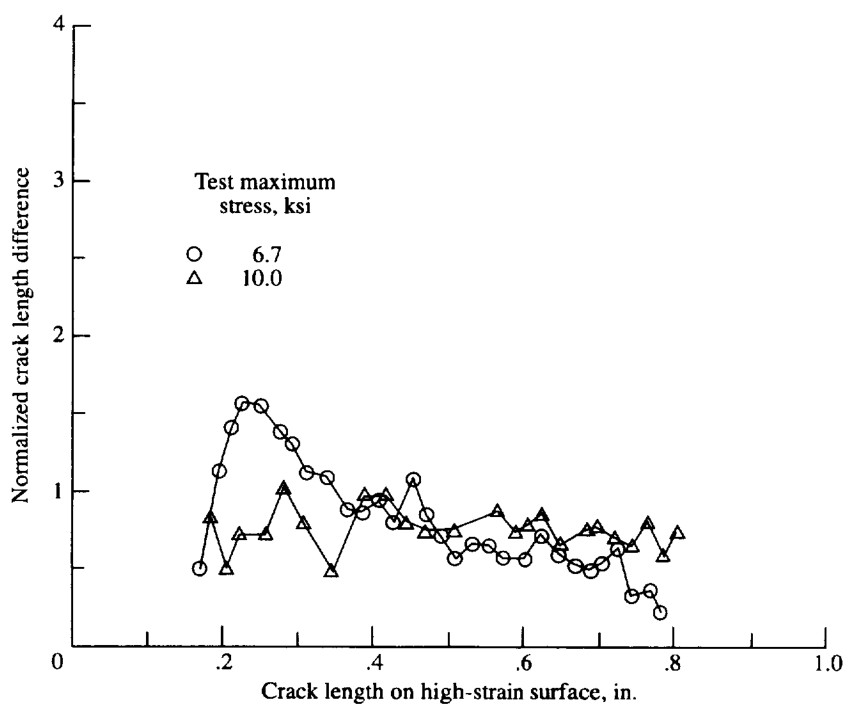

(b) B/M = 1.50.

Figure 4. Differences in crack length on two surfaces of 0.040-in.-thick specimens. Differences normalized by specimen thickness.

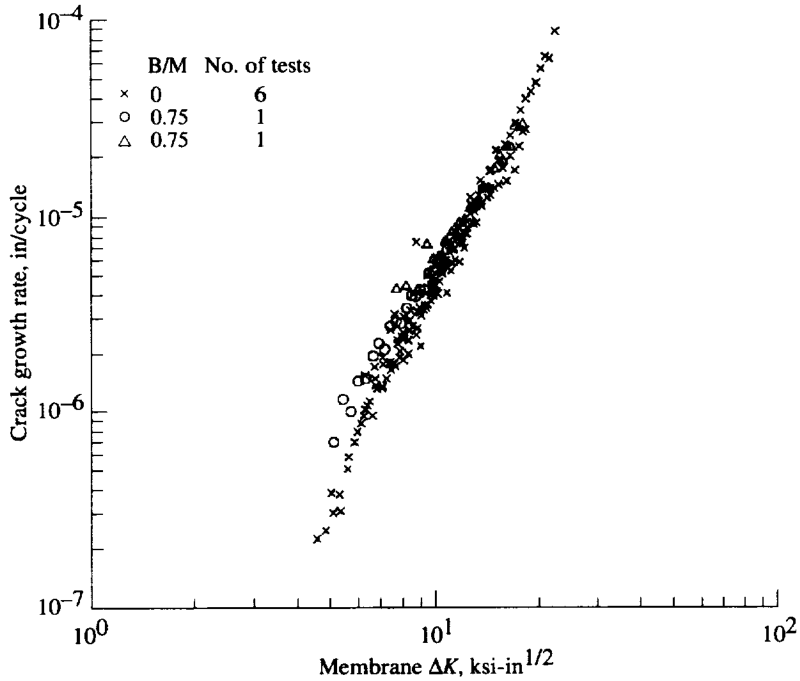

Figure 5. Fatigue crack growth rate data from tests of 0.040-in.-thick specimens with bending to membrane stress ratios of 0 and 0.75.

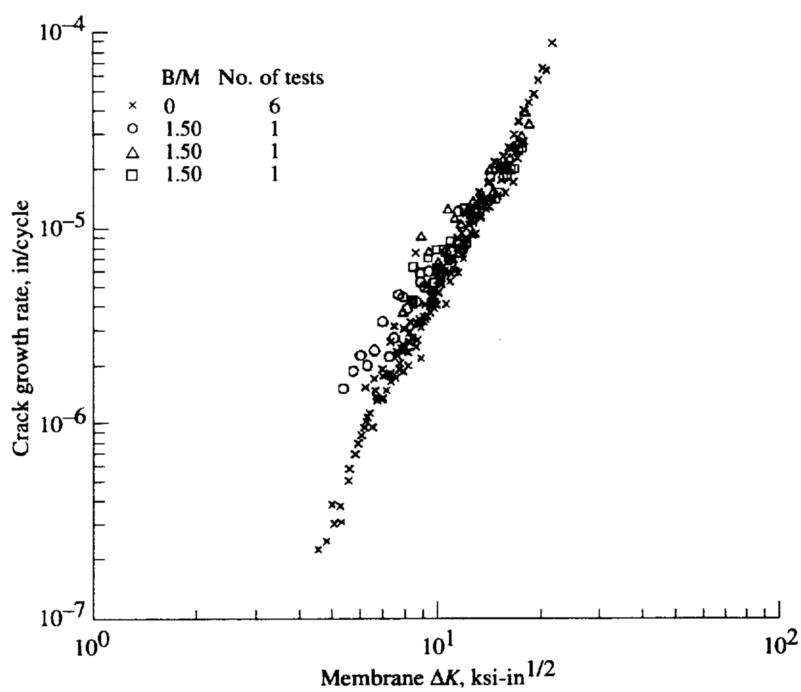

Figure 6. Fatigue crack growth rate data from tests of 0.040-in.-thick specimens with bending to membrane stress ratios of 0 and 1.50.

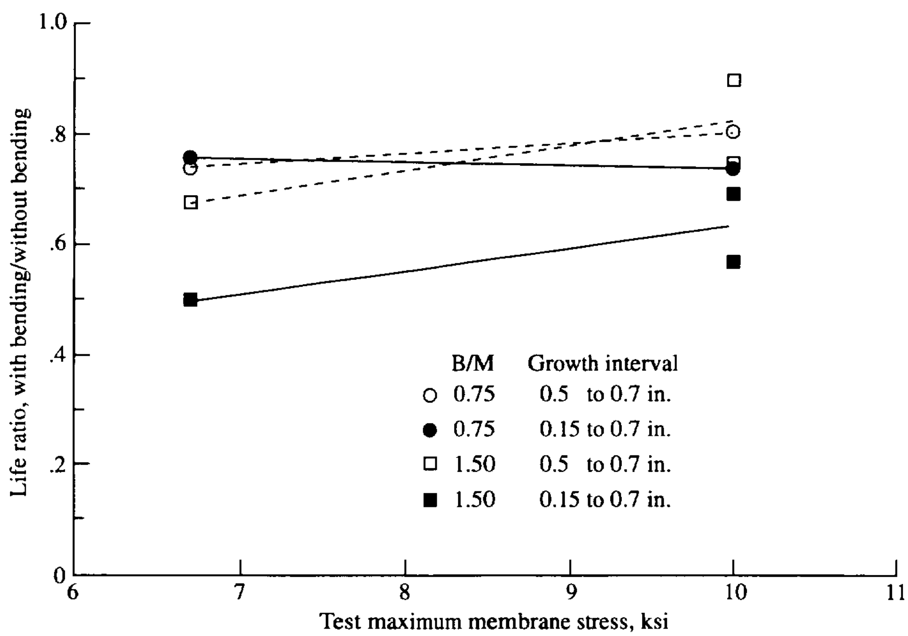

Figure 7. Effect of bending on lives of 0.040-in.-thick specimens.

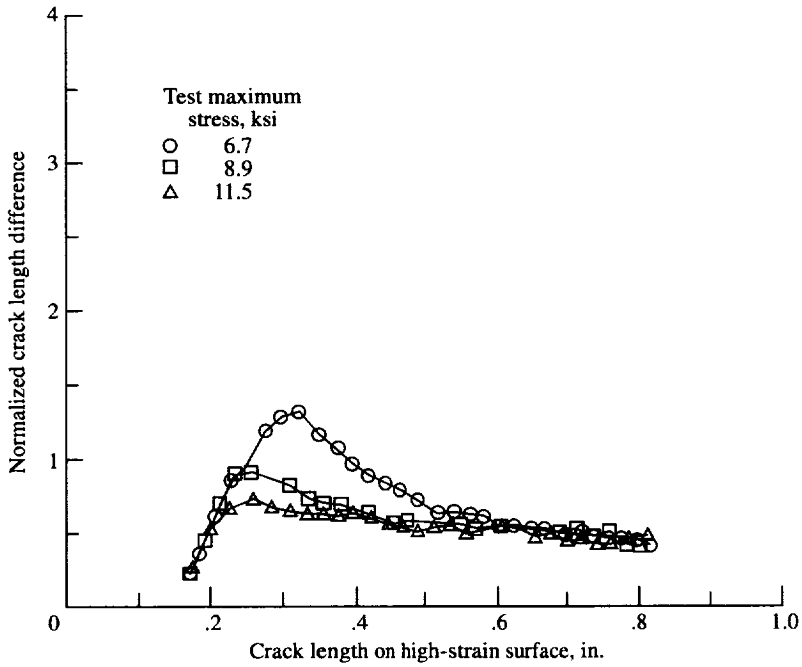

(a) B/M = 0.75.

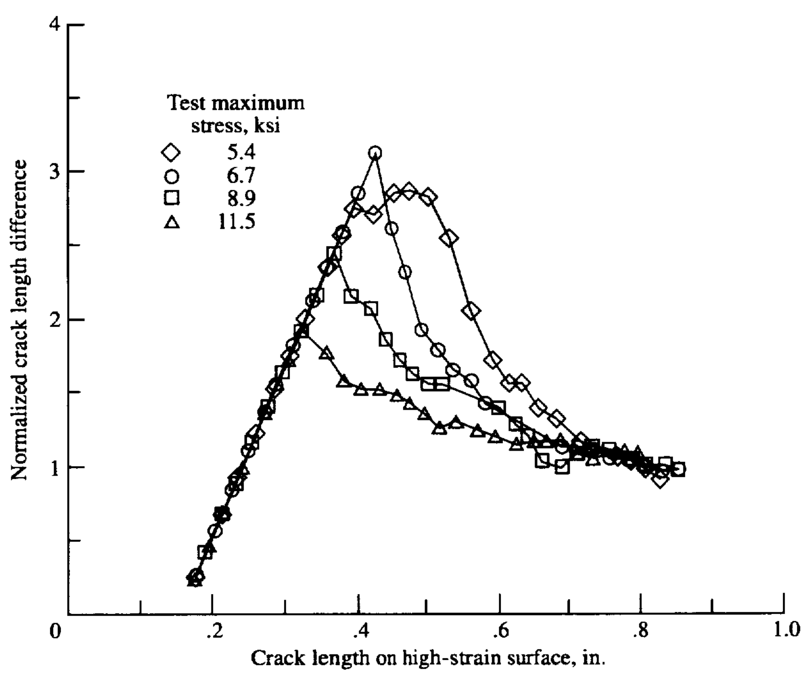

(b) B/M = 1.50.

Figure 8. Differences in crack length on two surfaces of 0.090-in.-thick specimens. Differences normalized by specimen thickness.

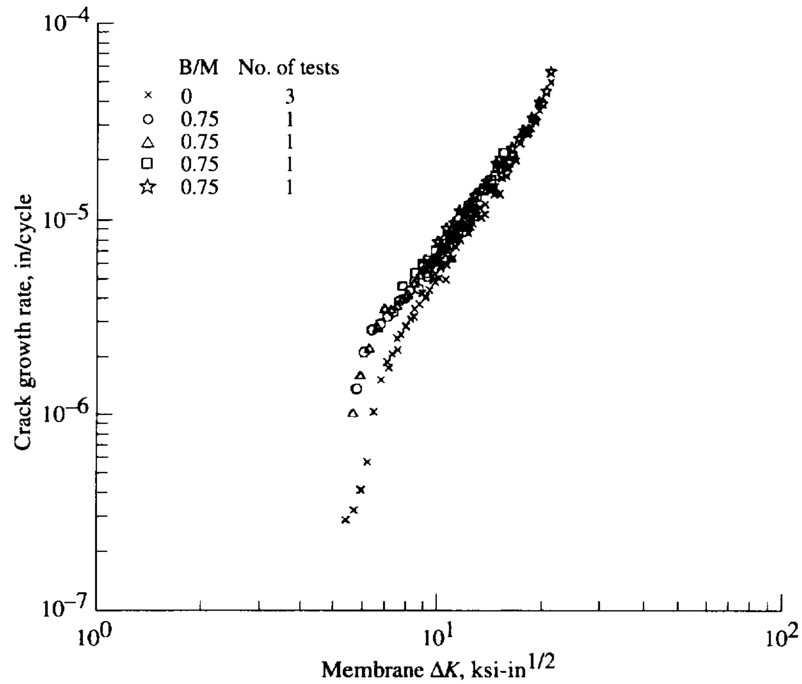

Figure 9. Fatigue crack growth rate data from tests of 0.090-in.-thick specimens with bending to membrane stress ratios of 0 and 0.75.

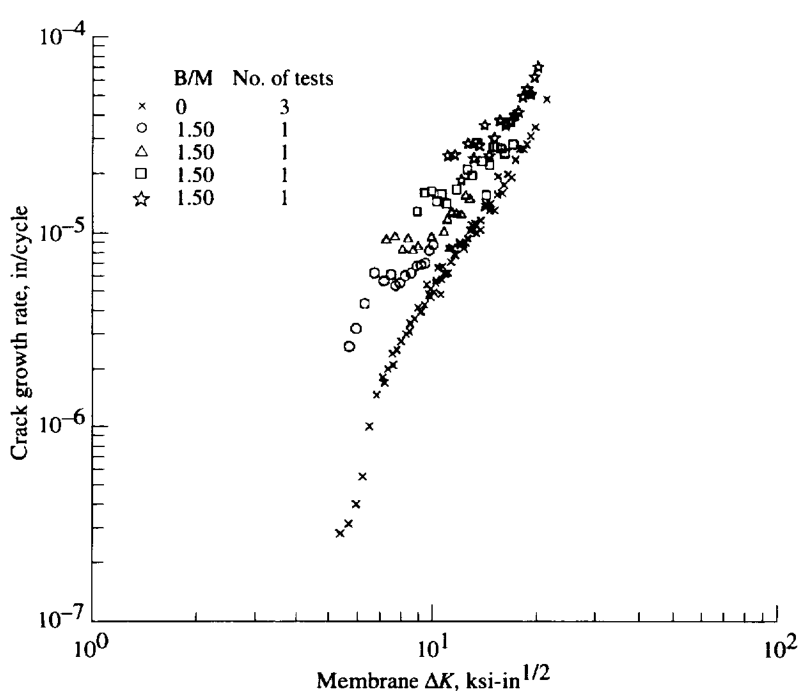

Figure 10. Fatigue crack growth rate data from tests of 0.090-in.-thick specimens with bending to membrane stress ratios of 0 and 1.50.

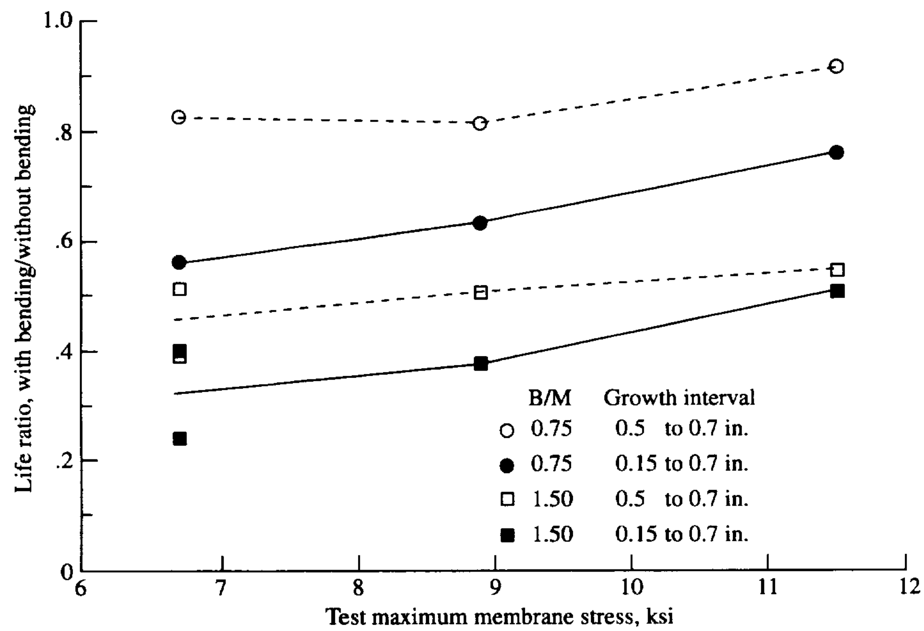

Figure 11. Effect of bending on lives of 0.090-in.-thick specimens.

REPORT DOCUMENTATION PAGE

Form Approved
OMB No. 0704-0188

1. AGENCY USE ONLY *(Leave blank)*

2. REPORT DATE
October 1997

3. REPORT TYPE AND DATES COVERED
Technical Memorandum

4. TITLE AND SUBTITLE
An Experimental Study of Fatigue Crack Growth in Aluminum Sheet Subjected to Combined Bending and Membrane Stresses

5. FUNDING NUMBERS
WU 538-02-10-01

6. AUTHOR(S)
Edward P. Phillips

7. PERFORMING ORGANIZATION NAME(S) AND ADDRESS(ES)
NASA Langley Research Center
Hampton, VA 23681-2199

8. PERFORMING ORGANIZATION REPORT NUMBER
L-17617

9. SPONSORING/MONITORING AGENCY NAME(S) AND ADDRESS(ES)
National Aeronautics and Space Administration
Washington, DC 20546-0001

10. SPONSORING/MONITORING AGENCY REPORT NUMBER
NASA TM-4784

11. SUPPLEMENTARY NOTES

12a. DISTRIBUTION/AVAILABILITY STATEMENT
Unclassified–Unlimited
Subject Category 39
Availability: NASA CASI (301) 621-0390

12b. DISTRIBUTION CODE

13. ABSTRACT *(Maximum 200 words)*

An experimental study was conducted to determine the effects of combined bending and membrane cyclic stresses on the fatigue crack growth behavior of aluminum sheet material. The materials used in the tests were 0.040-in.-thick 2024-T3 alclad and 0.090-in.-thick 2024-T3 bare sheet. In the tests, the membrane stresses were applied as a constant amplitude loading at a stress ratio (minimum to maximum stress) of 0.02, and the bending stresses were applied as a constant amplitude deflection in phase with the membrane stresses. Tests were conducted at ratios of bending to membrane stresses (B/M) of 0, 0.75, and 1.50. The general trends of the results were for larger effects of bending for the higher B/M ratios, the lower membrane stresses, and the thicker material. The addition of cyclic bending stresses to a test with cyclic membrane stresses had only a small effect on the growth rates of through-thickness cracks in the thin material, but had a significant effect on the crack growth rates of through-thickness cracks in the thick material. Adding bending stresses to a test had the most effect on the initiation and early growth of cracks and had less effect on the growth of long through-thickness cracks.

14. SUBJECT TERMS
Material fatigue; Metal fatigue; Crack propagation; Fatigue tests; Combined stress; Bending; Axial stress; Aluminum alloys

15. NUMBER OF PAGES
18

16. PRICE CODE
A03

17. SECURITY CLASSIFICATION OF REPORT	18. SECURITY CLASSIFICATION OF THIS PAGE	19. SECURITY CLASSIFICATION OF ABSTRACT	20. LIMITATION OF ABSTRACT
Unclassified	Unclassified	Unclassified	

NSN 7540-01-280-5500

Standard Form 298 (Rev. 2-89)
Prescribed by ANSI Std. Z39-18
298-102